

1 Article

2 An experimental and numerical study of the impact of ambient 3 light of SiPMs in VLC receivers

4 William Matthews ¹ and Steve Collins ^{2,*}

5 ¹ Department of Engineering Science, University of Oxford; william.matthews@eng.ox.ac.uk

6 ² Department of Engineering Science, University of Oxford; steve.collins@eng.ox.ac.uk

7 * Correspondence: steve.collins@eng.ox.ac.uk

8
9
10 **Abstract:** Silicon photomultiplier's relatively large area and ability to detect single photons makes
11 them attractive as receivers for visible light communications. However, their non-linear response has
12 a negative impact on the receiver performance, including making them particularly sensitive to amb-
13 ient light. Experiments and Monte Carlo simulations have been used to study this non-linearity.
14 The resulting detailed understanding of the origins of the non-linear response leads to concerns over
15 the accuracy of some previous simulations of SiPMs. In addition, it leads to simple methods to de-
16 termine the maximum rate at which a SiPM can count photons and of determining the impact of a
17 SiPMs non-linearity on its performance of a receiver. Finally, a method of determining which filters
18 should be used to protect a SiPM from ambient light is proposed.

19
20 **Keywords:** Visible Light Communications, SiPM, Monte Carlo

21
22
23
24
Citation: Lastname, F.; Lastname, F.;
Lastname, F. Title. *Photonics* 2022, 9,
x. <https://doi.org/10.3390/xxxxx>

Received: date 26
Accepted: date 27
Published: date 28

Publisher's Note: MDPI stays neutral with regard to jurisdictional claims in published maps and institutional affiliations. 29
30
31



32
33
34 **Copyright:** © 2022 by the author
35 Submitted for possible open access
36 publication under the terms and con-
37 ditions of the Creative Commons At-
38 tribution (CC BY) license (<https://creativecommons.org/licenses/by/4.0/>)

1. Introduction

Visible light communications (VLC) and optical wireless communications (OWC) have been proposed as approaches to increasing local wireless communications capacity using visible or optical wavelengths [1]. An important parameter for any communications system is the rate at which it makes errors. This is characterized by the bit error rate (BER), which depends upon the signal to noise ratio (SNR) at the output of the receiver. One approach to increasing the SNR of a VLC or OWC systems that are designed to operate at data rates of more than 100 Mbps is to use a silicon photomultiplier (SiPM) as a receiver [2-16]. These devices are arrays of microcells, containing a single photon avalanche diode (SPAD), and each microcell is designed so that an output pulse is generated whenever a photon initiates an avalanche event. It is the resulting ability to detect single photons which allows SiPM receivers to operate within a few photons per bit

39 of the noise floor determined by Poisson statistics [5]. However, an intrinsic
40 part of the microcell's photon detection mechanism is the quenching of the
41 avalanche process by reducing the bias voltage across its avalanche photo-
42 diode (APD). After the avalanche process has been quenched the microcell
43 has to be recharged so that another photon can be detected. Unfortunately,
44 this means that the SiPM has a non-linear response [4].

45 SiPMs are commercially available with different characteristics, in-
46 cluding area, numbers of microcells, photon detection efficiencies (PDEs),
47 recharge times and output bandwidths, which are expected to impact their
48 performance in receivers. The performance of receivers containing SiPMs
49 can be determined experimentally [3-7, 9-16]. However, these experiments
50 should be performed very carefully and are time consuming. In addition,
51 other parts of the system, particularly the transmitter, can have a signifi-
52 cant impact on the performance of a system. Furthermore, even when this
53 doesn't happen, it can be difficult to separate the impact of different SiPM
54 characteristics. Finally, it isn't always possible to test a receiver in some
55 environments, for example outside. These issues mean that a model or sim-
56 ulation of a SiPM receiver can complement experimental results.

57 Previously, SiPMs have been modelled using equivalent circuits or
58 Monte Carlo simulations [17]. However, numerical methods, including
59 Monte Carlo simulations, have been preferred when the performance of
60 SiPMs in receivers is modelled. Some Monte Carlo simulations have fo-
61 cussed upon the impact of the SiPM's non-linear response on their ability
62 to count photons [18]. However, this meant that it wasn't necessary to take
63 the finite width of the SiPMs output pulses into account. Furthermore, it
64 was assumed that a microcell can't detect photons whilst it is recovering
65 [18]. Alternatively, the performance of SiPM receivers has been studied by
66 evaluating relevant equations [19-22]. It should be possible to evaluate a
67 series of equations in less time than it takes to perform Monte Carlo simu-
68 lations. Unfortunately, sometimes these equations assume a feature, such
69 as a digital output, which aren't relevant to commercial SiPMs [19]. Alter-
70 natively, they are relevant to OFDM [22] which isn't as energy efficient as
71 on-off keying (OOK) [23] and currently gives a lower data rate than OOK
72 at eye safe irradiances [14]. In other cases the equations assume that, since
73 the microcells are passively quenched, they are paralysable [18,20]. This
74 assumption is correct when the microcells have a digital output [19], but,
75 commercial SiPMs have analog outputs and they are therefore not neces-
76 sarily paralysable. To create a simulation that is based upon the fewest
77 possible assumptions a Monte Carlo simulation of the physical processes
78 in a SiPM has been created.

79 The parameters in the simulation are obtained from either the relevant
80 data sheet or experimental results. The results of the simulations are then
81 validated by comparing them to results of experiments. In particular, they
82 are compared to measurements of the bias current needed to sustain an

83 over-voltage on the SiPM and the impact of ambient light on the perfor-
84 mance of receivers containing SiPMs. The simulation results are then used
85 to show that microcells are able to detect photons whilst they are recharg-
86 ing. The simulation results also lead to a new simple method of predicting
87 the impact of the non-linear response of the SiPM on receiver performance
88 in ambient light and a method for selecting optical filters that should be
89 used in receivers. In the future it should be possible to use the Monte-Carlo
90 simulation to devise an efficient means to compensation for any SiPM non-
91 linear caused by the transmitted data or to predict the performance of re-
92 ceivers containing existing or future SiPMs in a wide variety of situations.

93 This paper is organized as follows. Section 2 contains descriptions of
94 the operation of a SiPM, the experimental procedure used to test receivers
95 containing SiPMs and the Monte-Carlo simulation. This is followed in sec-
96 tion 3 by results of experiments to determine the voltage dependence of the
97 microcells PDE. This section also contains the results of experiments to de-
98 termine either the irradiance dependence of the current needed to sustain
99 an over-voltage or the impact of ambient light on the performance of re-
100 ceivers containing SiPMs. In both cases these experimental results are com-
101 pared to the results of Monte Carlo simulations of the same experiments.
102 Finally, section 4 contains results which show that microcells can detect
103 photons before they are fully charged. Results are also presented which
104 show that despite this behavior the maximum count rate of a SiPM can be
105 determined using an equation that was derived assuming that there was a
106 minimum time between photons that could be detected, a time previously
107 known as the dead time. The non-linear response of the SiPM is then
108 shown to arise from a combination of changes to the average PDE and mi-
109 crocell charge when photons are detected. This leads to a simple method
110 of predicting the impact of the SiPM's non-linearity on the performance of
111 a receiver in ambient light. Finally this section includes a suggested
112 method for selecting optical filters to use with SiPMs in receivers and a
113 discussion of the possible future uses of the Monte Carlo simulation.

114 2. Experimental Procedure and Monte-Carlo Simulation of SiPMs

115 2.1 Description of SiPM and their response to light

116 A silicon photomultiplier is an array of microcells that are connected
117 in parallel. Each microcell contains an APD which is biased above its break-
118 down voltage, $V_{\text{breakdown}}$, by an amount known as the over-voltage, V_{ov} . The
119 probability that an avalanche will occur [24] means that the PDE of a mi-
120 crocell can be calculated using

$$121 \quad PDE(\lambda, t) = PDE_{\text{max}}(\lambda) \times (1 - \exp(-V_{\text{ov}}(t)/V_{\text{char}})) \quad (1)$$

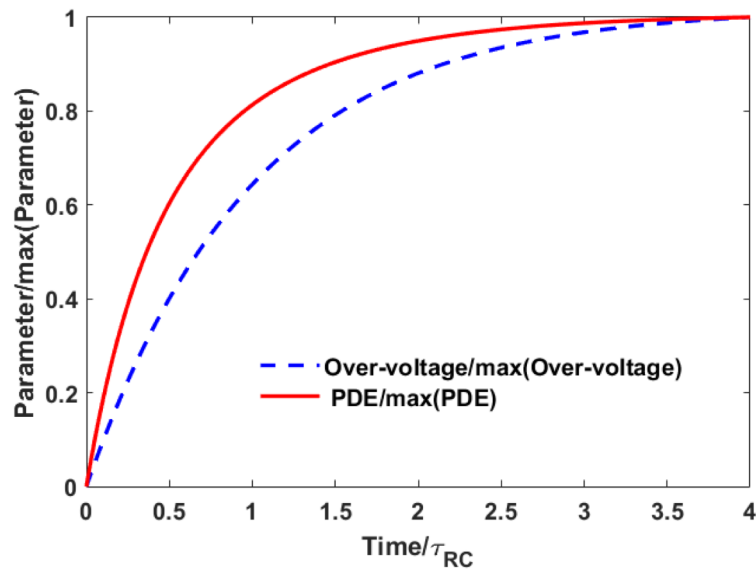


Figure 1. The recovery of the over-voltage and the photon detection efficiency determined using equations (1) and (2).

where $V_{ov}(t)$ is the instantaneous over-voltage, $PDE_{max}(\lambda)$ is the maximum possible PDE at a particular wavelength and V_{char} is a characteristic voltage at this wavelength for the APD.

If the over-voltage is positive and the microcell only contained an APD then a photon could initiate a self-sustained avalanche event. This means that only one photon could be detected. This avalanche event therefore has to be quenched so that other photons can be detected. In the case of the commercially available SiPMs manufactured by Broadcom, Hamamatsu and Onsemi a resistor is placed in series with the APD within each microcell. Consequently, the current due to an avalanche process results in a voltage drop across the resistor which reduces the voltage across the APD. Once this voltage equals the APDs breakdown voltage the self-sustained avalanche process is quenched. The capacitance in the microcell is then recharged via this resistor and the resistance between the microcell and the source of the SiPM bias voltage. This means that the recharging process can be represented by the equation

$$V_{ov}(t) = V_{ov}(1 - \exp(-t/\tau_{RC})) \tag{2}$$

where t is the time since the avalanche process was quenched and τ_{RC} is the time constant for the recharging process. This time constant can be determined from individual pulses that occur when photons are detected and is typically tens of nanoseconds. If the capacitance of the microcell is C_{cell} then the additional charge stored in the microcell will be $C_{cell} V_{ov}$. The results in figure 1 show that the sensitivity of the PDE to the over-voltage means

122
123
124
125
126
127
128
129
130
131
132
133
134
135
136
137
138
139
140
141
142
143
144

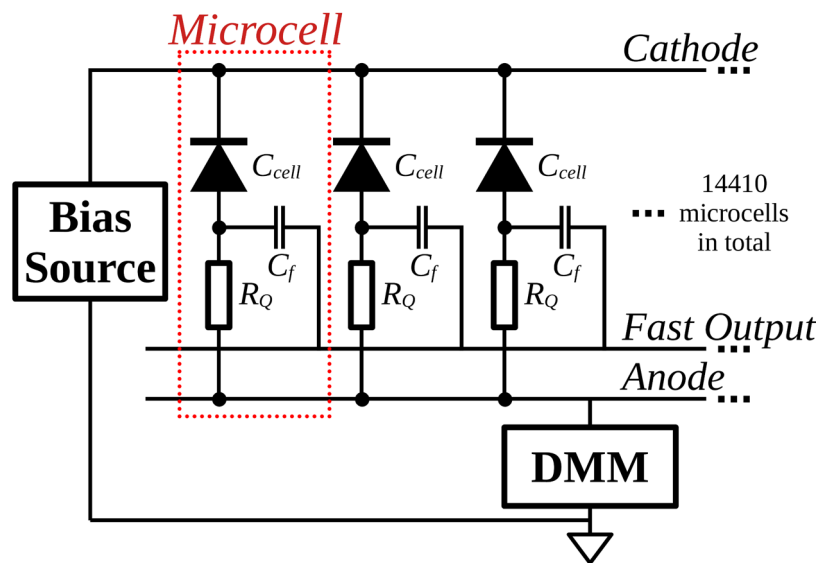


Figure 2. A schematic diagram showing three microcells in a representative Onsemi SiPM. The diagram also shows how these are connected the source of the bias voltage and a digital multimeter that is used to measure the bias current needed to sustain the bias voltage.

that it recovers more quickly than the over-voltage. Since the additional charge stored on the microcell is proportional to the over-voltage the PDE also recovers more quickly than the additional charge stored in the microcell.

Photons can be detected by monitoring the bias current that flows into the SiPM to recharge each microcell. This current flows because the microcell is discharged when it detects a photon, and since the amount of charge on the microcell is independent of the photon wavelength, the current is independent of the wavelength of the detected photon. If the interval between photons being detected by the SiPM is significantly longer than τ_{RC} then each detected photon results in a pulse with a fast rising edge followed by the exponential decay expected from equation (2). This mechanism can be used to detect and count photons using any of the commercially available SiPMs.

Figure 2 is a schematic diagram showing how a bias voltage was applied to a SiPM manufactured by Onsemi and a digital multimeter was connected to measure the current flowing to sustain this voltage. This figure also shows that these particular SiPMs have an output known as the

TABLE 1. KEY PARAMETERS OBTAINED FROM THE MANUFACTURES DATA SHEET FOR A J SERIES 30020 [26]

Parameter	30020
Number of microcells	14410
Microcells active area diameter (μm)	20
Fill factor (%)	62
Recharge/recovery time constant (ns)	15
Dark Count Rate (MHz)	1.2 (@ 5 V_{ov})
Fast output pulse width (ns)	1.4

145
146
147
148
149
150
151
152
153
154
155
156
157
158
159
160
161
162

163 fast output. In addition a second output can be created by placing a resistor
164 between the SiPM's anode and ground. This output is equivalent to the
165 output on SiPMs manufactured by other companies and it is possible to
166 detect individual photons using this output. However, the width of the
167 voltage pulses on this output is determined by the recharge time constant
168 of the microcells. Since this time is longer than the fast output pulse width,
169 this output is referred to as the slow output.

170 As shown in figure 2, the fast output is created by capacitively cou-
171 pling a common output to the connection between the APD and the
172 quenching resistor in each microcell [25]. This capacitive coupling means
173 that the signal on this fast output line is proportional to the rate of change
174 of the voltage across the APD. The charging of the node between the APD
175 and the resistor form the slow output pulses. This capacitance therefore
176 means that the pulses on the fast output are a high pass filtered version of
177 the slow output pulses. This removes the dc level component of the signal
178 and explains why the fast output pulses are at least an order to magnitude
179 narrower than the pulses on the slow output.

180 At low irradiances each microcell has time to recover before the next
181 photon is detected and the SiPM has a linear response. However, increas-
182 ing the irradiance falling on the microcells reduces the average time be-
183 tween successive photons passing through each microcell. Eventually pho-
184 tons arrive at microcells whilst they are still recharging. The result is that
185 the SiPM has a non-linear response. Previously, this non-linear response
186 has been observed by measuring the bias current needed to sustain the
187 over-voltage on the SiPM as the irradiance falling on the SiPM is increased
188 [10].

189 2.2. Experimental procedure

190 A schematic diagram of the equipment used to characterise the SiPM and
191 determine its performance as a VLC receiver is shown in figure 3. Previ-
192 ously, experiments were performed with J series SiPMs mounted on SMA
193 evaluation boards. These boards are convenient to use. However, they con-
194 tain a resistor in series with the SiPM so that slow output pulses can be
195 detected. Unfortunately, this resistor both increases the time needed for
196 each microcell to recharge and decreases the effective over-voltage, and
197 hence PDE, at high irradiances [16]. Since the fast output is used for data
198 transmission experiments this resistor isn't needed. More recently, experi-
199 ments have therefore been performed using a J series 30020 SiPM, whose
200 key characteristics are listed in table 1, mounted on a SMPTA board. With-
201 out a resistor in series with the SiPM, the SMTPA boards have a shorter
202 recharge time, and their PDE is not degraded at high ambient light levels.
203 This means a SiPM on a SMTPA board is both easier to model and, more
204 importantly, is a better receiver. As shown in figure 2, in the absence of a
205 resistor in series with the SiPM on the SMPTA board the current needed to

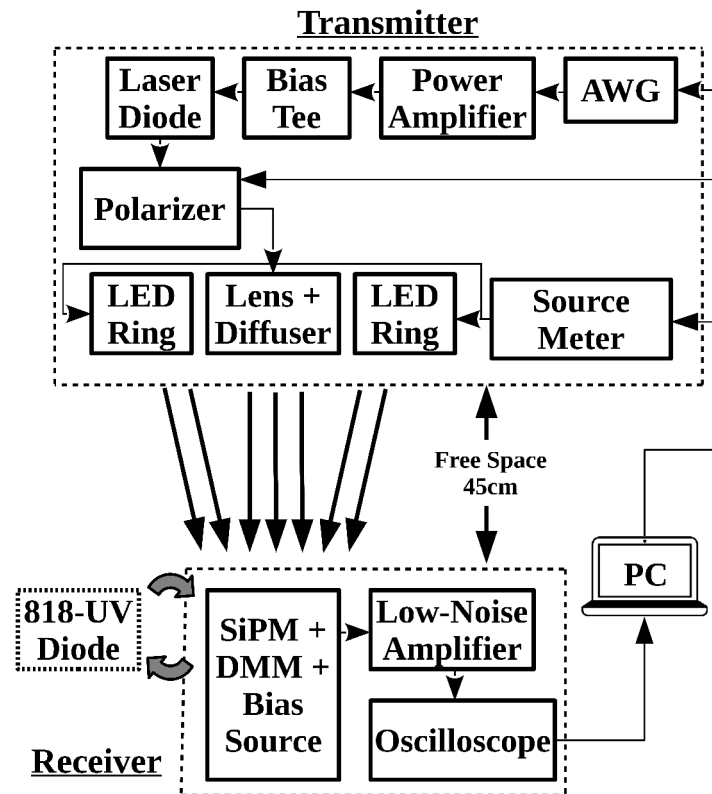


Figure 3. System block diagram describes the experimental setup used to evaluate the ambient light performance of the SiPM. The AWG was a 25GS/s AWG70002A, the Power Amplifier is a Fairview FMAM3269 10MHz to 6 GHz Amplifier which feeds a Bias Tee (Thorlabs ZFBT-4R2GW+) and the Laser Diode a ThorLabs L405P20. The LED ring includes eight UV3TZ-405-15 LEDs, which is driven by a Keithley 224 Source Meter. During some experiments the bias voltage applied to these 405 nm LEDs was varied to control the effective ambient light level. On the receiver side, the SiPM is coupled to a ZX60-43-S+ 4GHz Low Noise Amplifier which feeds a Keysight MSO64 (4GHz, 25GS/s) oscilloscope. The polarizer, source meter, AWG and oscilloscope are computer-controlled by MATLAB®.

sustain the over-voltage was measured with a Keithley 196 digital multi-meter.

To obtain reproducible results from data transmission experiments particular care had to be taken to minimize the impact of RF interference. When the beam from the transmitter to the receiver was blocked a 5 mV_{pp} interference signal was initially observed. Since the signal when a photon was detected was 15 mV_{pp} this level of interference was unacceptable. A near field probe was therefore used to determine that the source of the interference was the transmitter. The optical cage system containing the transmitter and the SMA cable connecting the transmitter to the AWG were therefore covered with a metallized cloth and the probe was then used to confirm that this cloth prevented this type of interference.

Even with this precaution it was sometimes impossible to obtain reproducible BER measurement results consistently. By watching the oscilloscope as it captured data it became clear that a 20 mV_{pp} signal occurred

206
207
208
209
210
211
212
213
214
215
216
217
218
219
220

frequently enough to explain the difficulties in reproducing results. A subsequent investigation showed that the frequency spectrum of this intermittent interference was consistent with it being caused by Wi-Fi and other RF signals transmitted by colleague's electronic devices. The experimental procedure was therefore changed so that any data captured when there was a significant level of this interference was discarded and the data transmitted again. However, there was so much interference during normal working hours that most results were captured overnight.

2.3. Monte-Carlo simulation of a SiPM

Results from experiments with a 30020 on a SMPTA board have been compared to results from a Monte-Carlo simulation of this SiPM. These simulations were performed with a time variable that increased by the minimum of one twentieth of a nanosecond and one twentieth of the bit time of the OOK data. Since the charge on the microcell and the microcell's recovery are independent of the detected photons wavelength, all the simulated photons are assumed to have the same wavelength as the transmitters output. This means that the impact of ambient light is represented by the irradiance at this wavelength which gives rise to the same count rate.

In some simulations the irradiance on the SiPM was assumed to be constant. However, when simulating data transmission experiments the irradiance was modulated to represent OOK data. At each time the instantaneous irradiance, the bit time and the Poisson probability density function

$$Poisson(n) = m^n e^{-m} / n! \quad (3)$$

were used to determine the number of photons incident on the SiPM in a bit time, n , where m is the mean of the distribution. At a time, t , this mean was calculated using

$$m(t) = (L_{TX}(t) + L_{amb}(t))A_{SiPM} \cdot dt / E_p \quad (4)$$

where $L_{TX}(t)$ is the irradiance from the transmitter at time t and $L_{amb}(t)$ is the irradiance representing ambient light at the same time. In addition, dt is the time step used in the simulation, E_p is the energy of a photon from the transmitter and A_{SiPM} is the area of the SiPM. The n photons calculated using (3) and (4) were then randomly distributed in the bit time. This was done using a random number with a Poisson distribution so that the time between photons had the required exponential distribution.

Once the photon stream had been generated an event-driven Monte-Carlo simulation was started and the following quantities were calculated:

(i) The total charge on all microcells.

$$Q_{total}(t) = \sum_{n=1}^{N_{cells}} C_{cell} V_{ov} (n, t) \quad (5)$$

where C_{cell} is the capacitance of a microcell and $V_{ov}(n,t)$ is the over-voltage on the n^{th} microcell at time t .

(ii) The average charge on the microcells that have detected a photon at this time. In this case (5) is evaluated, but, only the microcells that have detected a photon at this time are included in the summation. This sum is then divided by the number of microcells that have detected a photon at this time.

(iii) The instantaneous current needed to recharge each microcell was calculated by multiplying the increase in the over-voltage for each microcell since the previous time by the microcell capacitance and dividing the result by dt . The total current was then calculated by adding all these contributions, hence

$$I_{bias}(t) = \sum_{n=1}^{N_{cells}} \begin{cases} \frac{C_{cell}}{dt} (V_{ov}(n,t) - V_{ov}(n,t-dt)) & \text{if } V_{ov}(n,t) > V_{ov}(n,t-dt) \\ 0 & \text{otherwise} \end{cases} \quad (6)$$

(iv) The proportion of microcells that are fully charged was calculated by determining the proportion of microcells whose over-voltage is 99% of the maximum over-voltage.

(v) The average PDE of all the microcells was determined using (1) to determine the instantaneous PDE of each microcell and then calculating the average value.

The simulation started by initiating the microcells in the SiPM into a state that is consistent with the initial irradiance. The simulation was then evolved by up-dating the over-voltage and PDE of each microcell using equations (1) and (2) until the time at which the next photon or photons are incident on the SiPM. At each of these times the first step was to use a uniformly distributed random number to determine which microcell might detect the photon. The instantaneous PDE of the selected microcell and a second random number were then used to determine if the photon was detected. If the photon was detected the over-voltage and PDE of the microcell were both instantaneously set to zero. In addition, the charge on this microcell was added to the sum of the charge on microcells that had detected a photon at this time. This process was then repeated for all photons incident on the SiPM at the same time. Once the process of detecting photons at a particular time had been completed all the quantities of interest were calculated. The simulation was then evolved until the time when the next photon or photons were incident on the SiPM. This process was then repeated until the end of the simulated time.

At the end of the simulation the sum of the charge on microcells that detected photons at each time was convolved with a Gaussian kernel, which represented the shape of a fast output pulse. The result was a fast

output pulse whose integral is proportional to the charge discharged by all the photons detected at a particular simulated time. If the incident irradiance was modulated to represent OOK data the resulting simulated fast output was processed in the same way as the fast output from a SiPM in an experiment.

When writing the simulation a decision was made not to include three non-ideal behaviors of SiPMs, specifically dark counts, after-pulsing and optical cross-talk. Dark counts are spontaneous avalanche events that occur in the dark and in the 30020 they occur at a rate of 1 MHz[26]. This is much smaller than the anticipated rate at which ambient light photons are detected and so it wasn't included in the simulation. After-pulsing occurs when a charge carrier initiates an avalanche event in the same microcell after being temporarily trapped in the high field region of a microcell [17]. Similarly, cross-talk occurs when a secondary photon produced by an avalanche event initiates an avalanche in another microcell either immediately or after a delay [17]. In a 30020 the cross-talk occurs after less than 7.5% of avalanche events and after-pulsing after less than 5% of avalanche events. It isn't clear from this data if these effects needed to be included to achieve the required modelling accuracy. Furthermore, the data required to model the delays in these effects isn't provided by the manufacturer. The pragmatic decision was therefore taken to create a numerical model that excluded these effects and then reconsider this decision once its results had been compared to experimental data. The results in sections 3.3 and 3.4 suggest that it isn't necessary to include these effects in the Monte Carlo simulation.

3. Results

3.1. Photon detection efficiency measurement

One piece of important information required for an accurate Monte Carlo simulation of a SiPM is the relationship between PDE and over-voltage. Figure 4 shows PDE measurement results, obtained when the 405 nm irradiance on a 30020 J-series SiPM was constant at 2.4 mWm^{-2} , and the bias voltage varied. This irradiance was selected to stimulate avalanches at a rate which dominates the dark count rate, while remaining in the SiPM's linear region. The bias current at this irradiance and for each over-voltage, $I_{bias}(V_{ov}, L)$, was then measured and the PDE, $\eta(V_{ov}, \lambda)$, was then calculated using [16].

$$\eta(V_{ov}, \lambda) = \frac{E_p I_{bias}(V_{ov}, L)}{C_{cell} V_{ov} A_{SiPM} L} \quad (7)$$

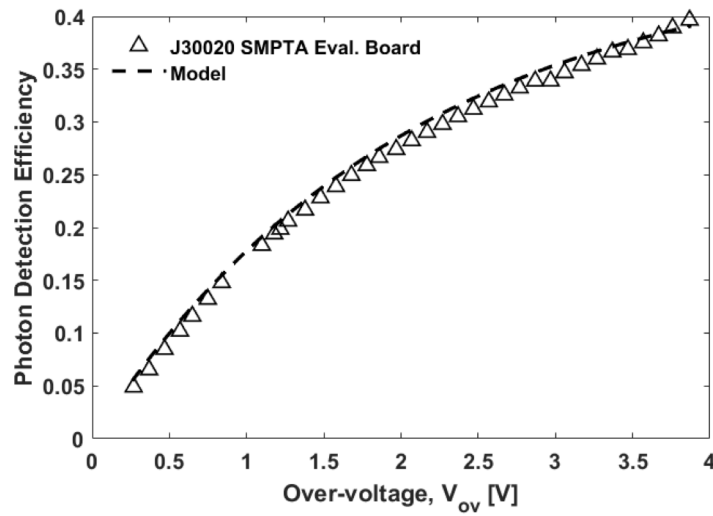


Figure 4. The photon detection efficiency of a J series 30020 SiPM on a SMPTA evaluation board measured at different over-voltages compared to equation (1).

In this figure the experimental results are compared to equation (1) with parameters $PDE_{max}(\lambda) = 0.46$ and $V_{char} = 2.03 V$. The excellent agreement between the experimental results and those predicted using these parameters meant that these parameters were used in Monte-Carlo simulations.

3.2. Measured bias current

Another key parameter in a simulation is the capacitance of the microcells. Since this is the capacitance of a reverse bias APD it may be voltage dependent. The bias current needed to sustain the voltage applied to the SiPM saturates when the time between detected photons is comparable to the microcell RC time constant. However, before saturation occurs this bias current is related to the rate at which photons are detected by

$$I_{bias} = C_{rate} \times C_{cell} \times V_{ov} \tag{8}$$

where C_{rate} is the rate at which photons are being counted, C_{cell} is the capacitance of a microcell and V_{ov} is the over-voltage.

For monochromatic light an irradiance, L , can be converted to a photon flux per unit area by dividing the irradiance by the energy of each photon, E_p . The number of photons per second incident on a SiPM can then be determined by multiplying the result by the area of the SiPM, A_{SiPM} . If $\eta(V_{ov}, \lambda)$ is the PDE of the SiPM at the wavelength of the incident light then at low irradiances, the count rate of photons is

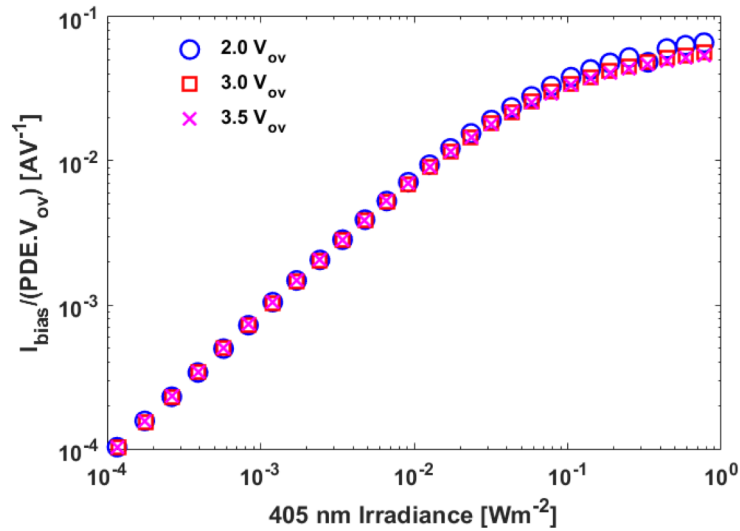


Figure 5. The measured current needed to sustain a bias on the SiPM at different irradiances of 405 nm light divided by the product of the over-voltage and the PDE corresponding to the over-voltage.

366

$$C_{rate} = \eta(V_{ov}, \lambda) A_{SiPM} L / E_p \tag{9}$$

367

Then if the capacitance of the microcell is independent of the over-voltage the resulting bias current is

368

369

$$I_{bias} = \eta(V_{ov}, \lambda) A_{SiPM} C_{cell} V_{ov} L / E_p \tag{10}$$

370

371

372

This equation shows that if the microcell capacitance is independent of over-voltage then at low irradiances the current will be proportional to the

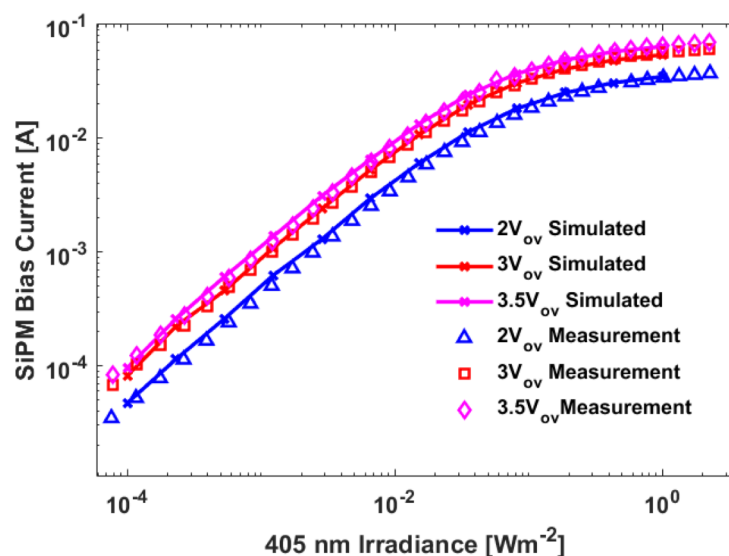


Figure 6. A comparison of the measured and simulated currents needed to sustain three different over-voltages on a 30020 SiPM.

product of the PDE and the over-voltage. Figure 5 shows the current measured at different over-voltages divided by the product of the over-voltage and the PDE at that over-voltage. The important conclusion from the results in this figure is that the microcell capacitance is independent of the over-voltage. Equation (10) and the measured bias current at low irradiances has therefore been used to determine the capacitance of each microcell. As shown in table 2 the resulting value, 46 fF, was one of the parameters used in the Monte Carlo simulation.

Table 2. Simulation Parameters for a J-Series 30020 SiPM

Parameter	30020
SiPM Area (mm ²)	9
Number of microcells	14410
V _{breakdown} (V)	24.5
V _{char} (V)	2.03 V
Maximum Photon Detection Efficiency at 405 nm	0.46
Recharge RC time constant (ns)	30.8
Microcell Capacitance (fF)	46
Full width at half maximum offast output pulse width (ns)	1.4
Simulation time step (s)	Maximum of (bit time)/20 and 0.05 ns

3.3. Comparison of measured and simulated bias currents

The voltage dependence of the photon detection efficiency and microcell capacitance obtained from experiment data have been incorporated into the Monte-Carlo simulation of the current needed to sustain over-voltages of 2.0 V, 3.0 V and 3.5 V. The results in figure 6 show an excellent agreement between these simulated current and the experimental results.

3.4 Data transmission experiments in ambient light

Figure 7 shows the results of experiments to determine the irradiance from the transmitter required to achieve a BER of 3.8×10^{-3} when the ambient light irradiance increases. Eye safe transmitters have been described providing a radius of horizontal coverage in a typical office of 2 m and which provide a minimum transmitter irradiance at 405 nm of 2 mWm^{-2} [11]. Figure 7 shows that with this transmitter irradiance, it is possible to support data rates up to 1.5 Gbps with a BER of 3.8×10^{-3} . However, as the data rate increases, the ambient light irradiance which may be tolerated decreases. In

particular, with a transmitter irradiance of 2mWm^{-2} , ambient irradiances of up to the equivalent of 1mWm^{-2} , 3mWm^{-2} and 5mWm^{-2} of 405nm light are tolerated at 1.5Gbps , 1Gbps , and 500Mbps .

The dominant noise source in a SiPM receiver is expected to be Poisson noise. If this is the case the BER when an on-off keyed signal is transmitted can be calculated using [5]

$$\text{BER} = \frac{1}{2} \left[\sum_{k=0}^{n_T} \frac{(N_{Tx}+N_b)^k}{k!} \cdot e^{-(N_{Tx}+N_b)} + \sum_{k=n_T}^{\infty} \frac{(N_b)^k}{k!} \cdot e^{-N_b} \right] \quad (11)$$

where N_b is the average number of photons detected per bit time when a zero is received, N_{Tx} is the number of additional detected photons per bit time needed from the transmitter when one is received and n_T is the threshold used to differentiate a one from a zero. The value of n_T that minimizes the BER has to be determined for particular combinations of N_b and N_{Tx} .

Equation (11) shows that the important parameters are the numbers of detected photons per bit when a zero and a one are received. These parameters have therefore been used as the axes in figure 8 to show the results of experiments during which the ambient light level, and hence the number of photons detected when a zero is transmitted, was varied. As expected from (11) using this x-axis the results for 500Mbps and 1000Mbps fall on the same curve. However, the results for 1500Mbps suggest that there is a relatively small, but noticeable, power penalty for this data rate. This may be caused by the width of the SiPM fast pulses or the limited bandwidth of another part of the link.

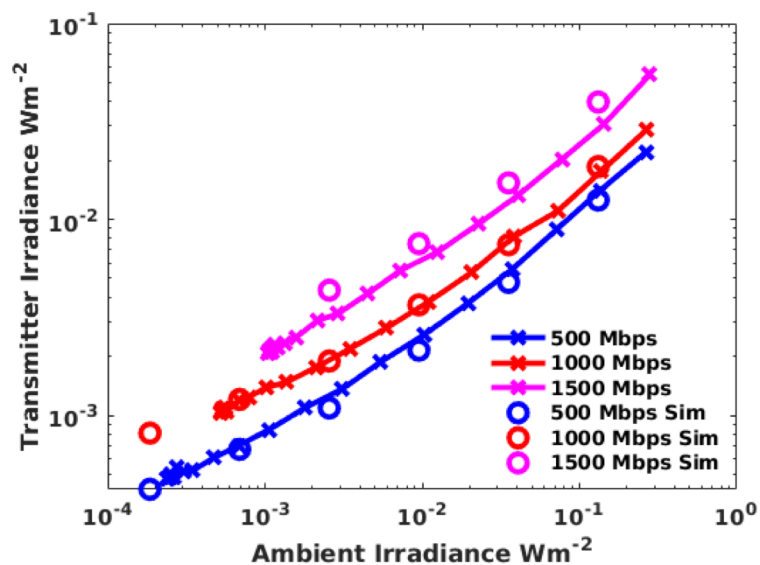


Figure 7. A comparison of the measured and simulated irradiances needed to support three data rates as the incident ambient light irradiance increased. The x axis is the equivalent 405nm irradiance that generates the same count rate and hence bias current as the incident ambient light.

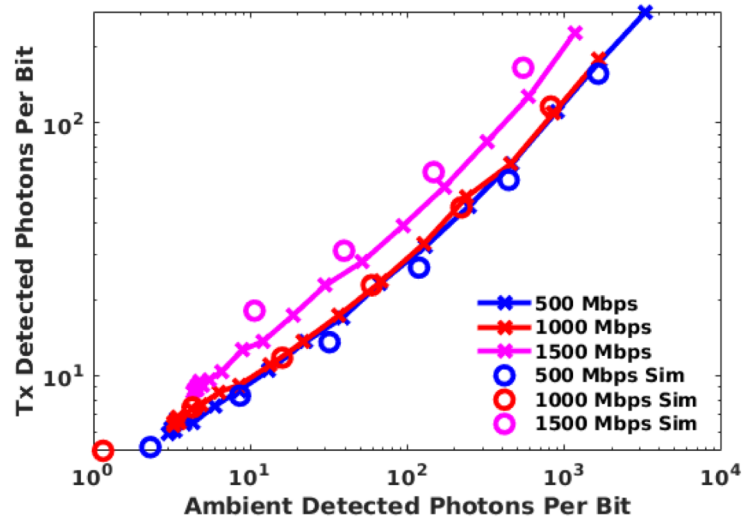


Figure 8. A comparison of the measured and simulated irradiances needed to support three data rates as the number of detected ambient light photons per bit time is increased.

In addition to the experimental results figure 8 also shows the results of Monte Carlo simulations of these experiments. Excellent agreement is obtained for data rates of 500 Mbps and 1000 Mbps. However, the agreement isn't as good for 1500 Mbps. The simulation included the width of the fast output pulses and the difference between the simulated 1000 Mbps and 1500 Mbps results shows that the width of the output pulses is starting to have an effect at data rates above 1000 Mbps. The difference between the results from experiments and the simulations at 1500 Mbps must therefore be due to something that hasn't been included in the simulations, for example the bandwidth of the transmitter. More importantly, the results in figure 8 confirm that, if the links performance is determined by the SiPM, then its performance can be predicted using this Monte Carlo simulation.

4. Discussion

4.1 The origins of the SiPMs non-linearity.

The count rate for a SiPM such as the 30020 can be related to the irradiance of monochromatic light falling on the SiPM, L , by [10]

$$C_{\text{rate}} = N_{\text{cells}} \alpha L / (1 + \alpha \tau_p L) \tag{12}$$

where N_{cells} is the number of microcells and τ_p is a characteristic time. In addition the parameter α is

$$\alpha = \frac{\eta(V_{ov}, \lambda) A_{\mu}}{E_p} \tag{13}$$

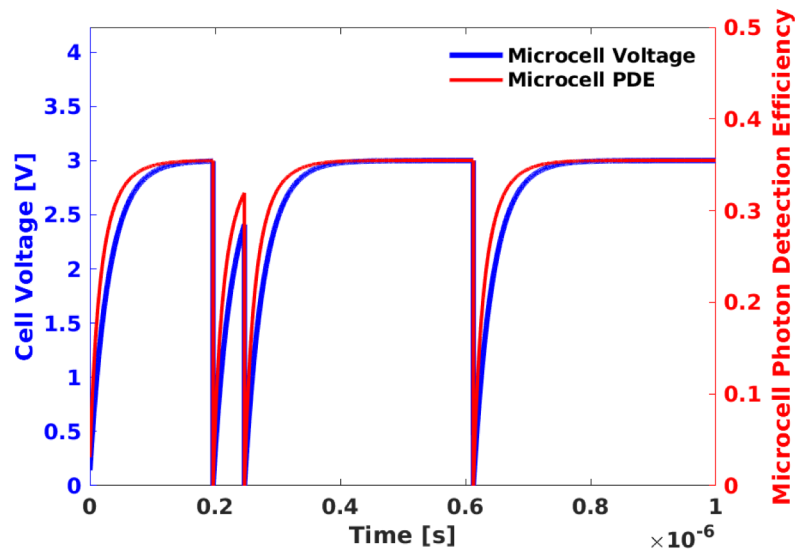


Figure 9. A representative microsecond of a simulation of one microcell showing the recovery of the over-voltage and PDE. In addition these results show an example, at approximately 0.25 μ s, of a photon being detected before the microcell is fully recharged

where $\eta(V_{ov}, \lambda)$ is the photon detection efficiency of the SiPM at a particular over-voltage and wavelength and V_{ov} , is the over-voltage E_p is the energy of each photon and A_μ is the active area of a microcell.

Equation (12) was suggested as a function which is consistent with the SiPM having a linear response at low irradiances and a saturated response at high irradiances. Furthermore, when (12) was suggested it was assumed that each microcell can't detect a photon whilst it was being recharged [4]. The latter assumption meant that previously the parameter τ_p was referred to as the dead-time for the microcell [4].

The assumption that a microcell can't detect a photon until it is fully recharged means that a charge $C_{cell} V_{ov}$ is discharged when a photon is detected. Consequently, the bias current needed to sustain the over-voltage is

$$I_{bias} = C_{cell} V_{ov} N_{cells} \alpha L / (1 + \alpha \tau_p L) \tag{14}$$

Previously, this equation has been shown to agree with experimental results [10]. It therefore appears that the assumption that a microcell can't detect a photon whilst it is recharging is correct and this assumption has been used to simulate SiPMs in receivers [19,27-28].

One advantage of developing a detailed Monte Carlo simulation is that it allows users to understand the physical processes occurring in microcells in detail. Figure 9 shows the behavior of a microcell when the average time between detected photons is longer than the time that the microcell needs to fully recharge. As expected in these circumstances the microcell is usually fully recharged before it detects a photon. However, the results in fig-

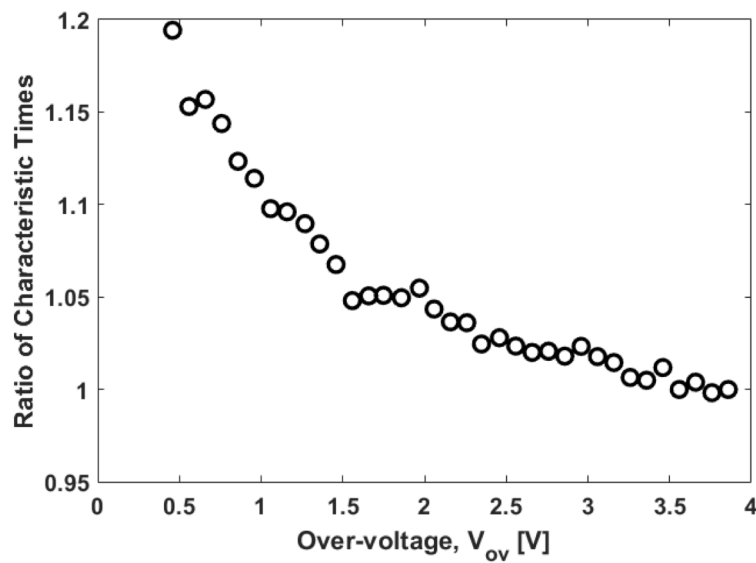


Figure 10. The ratio between the characteristic time obtained from the saturated current at each over-voltage to this time for an over-voltage of 3.85 V.

ure 9 show a photon being detected when the microcell is only partly recharged. This event clearly shows that, despite the concept of a dead time leading to an equation, equation (14), that fits the measured bias current data, microcells can detect photons when only partially recharged. Some conclusions arising from any simulations which assume that microcells are unable to detect photons whilst they are recharging will therefore be not be reliable. In addition, it should be possible to improve on any methods to compensate for the impact of the non-linearity which arise from these simulations.

4.2 A simple method of estimating the maximum count rate.

Although the concept of dead time, which was part of the derivation of (14), isn't accurate this equation has been shown to agree with measured bias current data. An important aspect of the derivation of equation (14) [4] was that it assumed that there was a minimum time between photons that a microcell could detect, τ_p . However, this parameter wasn't related to the recharge time of the microcell and it was therefore used to fit (14) to a particular set of experimental data.

The reason why it has previously been possible to show agreement between (14) and experimental results can be understood by considering the current flowing when the SiPM response saturates. Saturation occurs when the denominator of (14) is dominated by the second term and the resulting current when the SiPM saturates is

$$I_{sat} = N_{cells} C_{cell} V_{ov} / \tau_p \tag{15}$$

This means that

$$(I_{sat}(V_{ov1})/V_{ov1}) / (I_{sat}(V_{ov2})/V_{ov2}) = \tau_p(V_{ov2}) / \tau_p(V_{ov1}) \tag{16}$$

Consequently, the ratio of characteristic times needed to fit (14) to bias currents measured at different over-voltages can be determined from (16). This ratio of characteristic times has been determined for a wide range of over-voltages. The results in figure 10 show that, once the over-voltage is more than 1.5 V, this characteristic time is almost constant. This means that, for the range of over-voltages that are typically used, the maximum count rate of a SiPM can be estimated using

$$C_{\max} = N_{\text{cells}}/\tau_p \tag{17}$$

where τ_p is approximately 2.2 times the RC time constant of the micro-cells [10].

4.3 A simple method of predicting the impact of ambient light

The results in figures 7 and 8 show that the results of the Monte Carlo simulations can be used to predict the results of data transmission over a wide range of ambient light conditions. However, each simulation can take an inconvenient time. An even simpler prediction method would therefore be advantageous. The experimental results for the two data rates, 500 Mbps and 1000 Mbps, for which the VLC systems performance is determined by the SiPM alone are shown in figure 11. This figure also includes the performance of these systems predicted using the SiPM parameters and (11). The results in this figure show that the performance of the SiPM receiver at 500 Mbps and 1000 Mbps can be predicted using Poisson statistics until approximately 100 detected ambient light photons per bit. However, by 1000 detected ambient light photons per bit there is an error of a factor of approximately 2 in the prediction. If the photon detection efficiency is 0.35

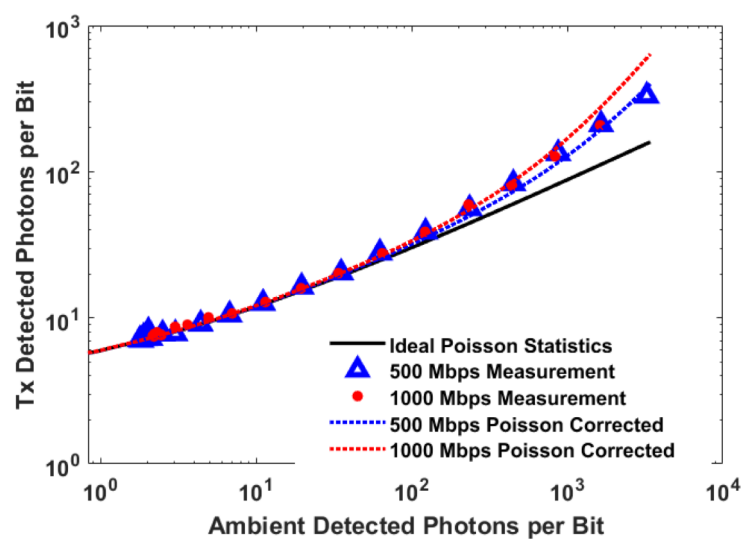


Figure 11. Experimental results for 500 Mbps and 1000 Mbps compared to the results expected from Poisson Theory and these results combined with the correction, equation (18). The x axis is the equivalent 405 nm irradiance that generates the same count rate and hence bias current as the incident ambient light.

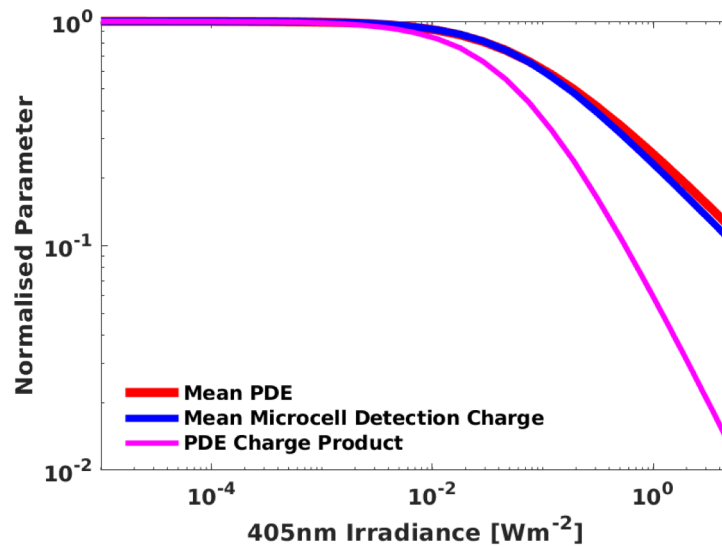


Figure 12. The mean array PDE when photons are detected and the mean charge on the microcells that have detected a photons.

513 then 1000 detected photons per bit corresponds to an irradiance of
 514 78 mWm⁻².

515 Figure 9 shows that photons can be detected before a microcell is fully
 516 charged and, hence whilst the microcells PDE is less than its maximum
 517 value. Furthermore, as the irradiance increases, more microcells will detect
 518 photons whilst their PDE is less than the maximum. The average PDE of
 519 the array at times when photons are detected has been calculated for dif-
 520 ferent simulated irradiances. The results in figure 12 show that, as expected,
 521 when the irradiance is high enough this array average PDE when any pho-
 522 ton is detected decreases. This change in the array average PDE alone
 523 might explain the non-linear response of the SiPM. However, the irradi-
 524 ance at which the array average PDE falls to half its maximum value is
 525 193 mWm⁻². In contrast, the current falls to half the value expected from its
 526 linear response when the irradiance is 73.6 mWm⁻². The change in the array
 527 average PDE when photons are detected can't therefore be the only mech-
 528 anism contributing to the SiPMs non-linear response.

529 An important assumption in the Monte Carlo simulation is that the
 530 height of the fast output pulse generated when a photon is detected is pro-
 531 portional to the charge on the microcell when that photon is detected. This
 532 means that the smaller charge stored on a microcell when it detects a pho-
 533 ton before it is fully recharged may be contributing to the non-linear re-
 534 sponse of both the bias current and the fast output used when the SiPM is
 535 a receiver. This may explain why the irradiance at which the transmitters
 536 sensitivity is half the expected value, 78 mWm⁻², is similar to the irradiance
 537 at which the measured bias current is half the expected value.

538 It appears that the charge stored when a photon is detected is contrib-
539 uting to the SiPMs non-linearity. The average charge stored on a microcell
540 when it detects a photon has therefore been calculated at different irradi-
541 ances. The results in figure 12 show that this effect is as significant as the
542 change in the array average PDE when a photon is detected. Consequently,
543 when the two processes are taken into account the average signal per inci-
544 dent photon falls to half its maximum value at an irradiance of 65 mWm^{-2} ,
545 which is much closer to the irradiance at which the bias current is half the
546 value expected from its linear response

547 The origin of the fast output pulses and the results in figure 12 suggest
548 that the non-linearity in the bias current should also have an impact on the
549 performance of the SiPM as a receiver. In this case the impact of the non-
550 linear SiPM response on the performance of a VLC system can be predicted
551 by multiplying the predictions from Poisson statistics by a correction factor

$$1 + \alpha \tau_p L \quad (18)$$

552
553 The results in figure 11 show that with this correction the experimental re-
554 sults for 500 Mbps and 1000 Mbps can be predicted accurately under a wide
555 range of ambient light conditions.

556 *4.4 Selecting optical filters for operation in ambient light*

557 Results such as those in figure 7 show that even in the presence of a signif-
558 icant amount of ambient light data rates up to at least 1500 Mbps can be
559 received. However, the noise added by the ambient light increases the ir-
560 radiance from the transmitter required to achieve a particular combination
561 of BER and data rate. In addition, at high ambient light irradiances the non-
562 linear response of the SiPM can cause an additional increase in the required
563 transmitter irradiance. This means that the SiPM should be protected from
564 ambient light using optical filters.

565 In the past optical filters with narrow pass-bands have been used to
566 protect SiPMs from ambient light [5,6,10]. However, they restrict the re-
567 ceiver's field-of-view. Consequently, optical filters which absorb light and
568 which support wider fields of view are preferred [11]. The first priority
569 when selecting filters should be to limit the impact of the SiPMs non-line-
570 arity. Equation (18) is valid for monochromatic light and the equivalent
571 equation for ambient light would need to take into account the spectrum
572 of the ambient light and the wavelength dependence of the SiPMs PDE.
573 However, this non-linearity affects the bias current. Consequently the ef-
574 fectiveness of filters can be determined by measuring the bias current for
575 a particular SiPM and ambient light source when different filters, or com-
576 binations of filters, are placed in front of the SiPM. If the ambient light is
577 strong enough to force the SiPM into its non-linear region the first priority
578 is to use filters that reduce its impact so that the impact of the SiPM's non-

579 linearity is reduced. The non-linearity will double the required transmitter
580 irradiance when

$$581 \quad \alpha \tau_p L_{\text{eff}} = 1 \quad (19)$$

582 where L_{eff} is the 405 nm irradiance that gives the same bias current as the
583 ambient light. At this irradiance the bias current is half the maximum bias
584 current. The first aim should be to ensure that the non-linearity increases
585 the required transmitter irradiance by a factor of two or less. This means
586 reducing the measured bias current to less than half its maximum value.
587 However, if the bias current can be reduced to less than one tenth of its
588 maximum value then the non-linearity is only increasing the required irra-
589 diance by approximately 10%, and may therefore be considered negligible.

590 A potential problem with aiming to reduce the bias current using fil-
591 ters is that it may require filters that also attenuate the wavelength used to
592 transmit data. Even when filters are used in high levels of ambient light the
593 number of detected photons per bit will probably be high enough for the
594 Poisson distribution to be approximately by a normal distribution. If this
595 is the case the noise caused by the ambient light will be proportional to the
596 square-root of the rate at which ambient light photons are detected. This
597 means that if using a filter reduces the bias current by a factor of $1/n$ then
598 the signal to noise ratio, and hence bit error rate, will be maintained if the
599 filter also reduces the bias current from the transmitter alone by a factor of
600 $1/\sqrt{n}$. This means that it isn't always necessary to use optical filters which
601 transmit all of the photons from the transmitter.

602 *4.5 Future work*

603 In the future understanding of the origins of the SiPMs non-linear response
604 obtained from Monte-Carlo simulations could be used to develop methods
605 to accommodate this non-linear when it is caused by the transmitted data
606 rather than by ambient light. This situation will most often arise when or-
607 thogonal frequency division multiplexing (OFDM) is used as a modulation
608 scheme. In OFDM data is transmitted by modulating several orthogonal
609 carriers. This increases the amount of data that can be transmitted in the
610 systems bandwidth. However, adding subcarriers means that OFDM has a
611 high peak transmitted power. Furthermore, the process of separating the
612 subcarriers relies upon the assumption that the system has a linear re-
613 sponse. At the moment the state-of-the-art method of dealing with the
614 SiPM non-linearity when OFDM is employed is to use a Volterra series
615 non-linear equalizer [13,14]. However, this standard adaptive method re-
616 lies upon a large number of parameters. In the future, the understanding
617 of the origins of the SiPMs non-linearity arising from the Monte Carlo sim-
618 ulations might lead to the development of a specific method to deal with
619 the SiPM non-linearity when OFDM is being used. This would hopefully

620 be simpler to implement and/or improve the systems performance when
621 compared to the existing state of the art.

622 If SiPMs become the photodetectors of choice in receivers then manu-
623 facturers will need to determine the relative importance of SiPM param-
624 eters such as PDE, number of microcells, recovery time and output pulse
625 width. The impact of these parameters could be investigated experimen-
626 tally using those SiPMs that are already commercially available. However,
627 experiments are difficult to perform reliably, the available SiPMs represent
628 a small range of possible parameter values and other parts of the system,
629 in particular the transmitter, can have an impact on the experimental re-
630 sults. These considerations mean that the best way to compare the perfor-
631 mance of SiPMs with different parameter combinations is using a detailed
632 numerical simulation which has been shown to generate results which
633 agree with experimental results.

634 **Funding:** This research has been supported by the UK Engineering and
635 Physical Sciences Research Council (EPSRC) under Grant EP/R00689X/1.

637 References

- 638 1. H. Haas, J. Elmirghani and I. White, "Optical Wireless Communication" *Philosophical Transactions of the Royal Society A*, **2020**
639 vol. 378.
- 640 2. M. Khalighi, T. Hamza, S. Bourennane, P. Léon and J. Opderbecke, "Underwater Wireless Optical Communications Using
641 Silicon Photo-Multipliers", *IEEE Photonics Journal*, **2017**, vol. 9, no. 4, pp. 1-10.
- 642 3. Leon, P., Roland, F., Brignone, L., Opderbecke, J., Greer, J., Khalighi, M.A., Hamza, T., Bourennane, S. and Bigand, M., "A
643 new underwater optical modem based on highly sensitive Silicon Photomultipliers," *OCEANS 2017*, Aberdeen, UK 19-22
644 June 2017
- 645 4. L. Zhang, D. Chitnis, H. Chun, S. Rajbhandari, G. Faulkner, D. O'Brien, and S. Collins, "A comparison of APD- and SPAD-
646 based receivers for visible light communications", *J. Lightw. Technol.*, **2018**, vol. 36, no. 12, pp. 2435–2442.
- 647 5. Z. Ahmed, L. Zhang, G. Faulkner, D. O'Brien and S. Collins, "A Shot-Noise Limited 420 Mbps Visible Light
648 Communication System using Commercial Off-the-Shelf Silicon Photomultiplier (SiPM)," 2019 IEEE International
649 Conference on Communications Workshops (ICC Workshops), Shanghai, China, 20-24 May 2019.
- 650 6. Z. Ahmed, R. Singh, W. Ali, G. Faulkner, D. O'Brien and S. Collins, "A SiPM-Based VLC Receiver for Gigabit
651 Communication Using OOK Modulation", *IEEE Photonics Technology Letters*, **2020**, vol. 32, no. 6, pp. 317-320.
- 652 7. L. Zhang, X. Tang, C. Sun, Z. Chen, Z. Li, H. Wang, R. Jiang, W. Shi, and A. Zhang, "Over 10 attenuation length gigabits per
653 second underwater wireless optical communication using a silicon photomultiplier (SiPM) based receiver," *Opt. Exp.*, **2020**,
654 vol. 28, no. 17, p. 24968.
- 655 8. M. A. Khalighi, H. Akhouayri and S. Hranilovic, "Silicon-Photomultiplier-Based Underwater Wireless Optical
656 Communication Using Pulse-Amplitude Modulation", *IEEE Journal of Oceanic Engineering*, **2020**, vol. 45, no. 4, pp. 1611-
657 1621.
- 658 9. Tang, X., Zhang, L., Sun, C., Chen, Z., Wang, H., Jiang, R., Li, Z., Shi, W. and Zhang, A. "Underwater Wireless Optical
659 Communication Based on DPSK Modulation and Silicon Photomultiplier," *IEEE Access*, **2020**, vol. 8, pp. 204676-204683.
- 660 10. W. Matthews, Z. Ahmed, W. Ali and S. Collins, "A 3.45 Gigabits/s SiPM-Based OOK VLC Receiver", *IEEE Photonics
661 Technology Letters*, **2021**, vol. 33, no. 10, pp. 487-490.
- 662 11. W. Ali, G. Faulkner, Z. Ahmed, W. Matthews and S. Collins, "Giga-Bit Transmission between an Eye-Safe Transmitter and
663 Wide Field-of-View SiPM Receiver", *IEEE Access*, **2021**, vol. 9, pp. 154225-154236.
- 664 12. Y. Li, Y. Hua, R. K. Henderson and D. Chitnis, "A Photon Limited SiPM Based Receiver for Internet of Things," *2021 Asia
665 Communications and Photonics Conference (ACP)*, Shanghai, China, 24-27 October 2021.
- 666 13. L. Zhang, R. Jiang, X. Tang, Z. Chen, J. Chen and H. Wang, "A Simplified Post Equalizer for Mitigating the Nonlinear
667 Distortion in SiPM Based OFDM-VLC System", *IEEE Photonics Journal*, **2022**, vol. 14, no. 1, pp. 1-7.

- 668 14. S. Huang, C. Chen, R. Bian, H. Haas, and M. Safari, "5 Gbps optical wireless communication using commercial SPAD array
669 receivers", *Opt. Lett.*, **2022**, vol. 47, pp. 2294-2297.
- 670 15. Li, Y., and Chitnis, D. "A real-time SiPM based receiver for FSO communication.", *SPIE Opto*, San Francisco, California,
671 United States, 3 March 2022.
- 672 16. W. Matthews and S. Collins, "The negative impact of anode resistance on SiPMs as VLC receivers," *2022 17th PRIME*
673 *Conference, Sardinia, Italy*, 12-15 June 2022.
- 674 17. F. Acerbi, and S. Gundacker, "Understanding and simulating SiPMs", in *Nuclear Instruments and Methods in Physics*
675 *Research Section A: Accelerators, Spectrometers, Detectors and Associated Equipment*, vol. 926, pp. 16-35, May 2019.
- 676 18. Gnecci, S., Dutton, N.A., Parmesan, L., Rae, B.R., McLeod, S.J., Pellegrini, S., Grant, L.A. and Henderson, R.K., "A
677 Simulation Model for Digital Silicon Photomultipliers," *IEEE Transactions on Nuclear Science*, **June 2016**, vol. 63, no. 3, pp.
678 1343-1350.
- 679 19. He C., Ahmed Z. and Collins S., "Signal Pre-Equalization in a Silicon Photomultiplier-Based Optical OFDM System," *IEEE*
680 *Access*, **2021**, vol. 9, pp. 23344-23356.
- 681 20. Huang, S., and Safari, M., "Hybrid SPAD/PD Receiver for Reliable Free-Space Optical Communication," *IEEE Open Journal*
682 *of the Communications Society*, **2020**, vol. 1, pp. 1364-1373.
- 683 21. Huang S., and M. Safari, S., "SPAD-Based Optical Wireless Communication With Signal Pre-Distortion and Noise
684 Normalization," *IEEE Transactions on Communications*, **2022**, vol. 70, no. 4, pp. 2593-2605.
- 685 22. Zhang, L., Jiang, R., Tang, X., Chen, Z., Li, Z., & Chen, J. "Performance Estimation and Selection Guideline of SiPM Chip
686 within SiPM-Based OFDM-OWC System.", *Photonics*, **September 2022**, Vol. 9, No. 9, p. 637.
- 687 23. Hinrichs, M., Berenguer, P.W., Hilt, J., Hellwig, P., Schulz, D., Paraskevopoulos, A., Bober, K.L., Freund, R. and Jungnickel,
688 V., A physical layer for low power optical wireless communications. *IEEE Transactions on Green Communications and*
689 *Networking*, 2020, 5(1), pp.4-17.
- 690 24. N. Otte, D. Garcia, T. Nguyen, and D. Purushotham, "Characterization of Three High Efficiency and Blue Sensitive Silicon
691 Photomultipliers", *Nucl. Instrum. Methods Phys. Res. Sect. Accel. Spectrometers Detect. Assoc. Equip.*, **2017**, vol. 846, pp. 106–
692 125.
- 693 25. Onsemi.com 2022. *Introduction to the Silicon Photomultiplier (SiPM) AND9770/D*
694 <https://www.onsemi.com/pub/Collateral/AND9770-D.PDF> (Accessed on 8th November 2022).
- 695 26. Onsemi.com. 2020. *J-Series SiPM Sensors Datasheet*. <https://www.onsemi.com/pub/Collateral/MICROJ-SERIES-D.PDF>,
696 (Accessed on 20 June 2022).
- 697 27. C. He and Y. Lim, "Silicon Photomultiplier (SiPM) Selection and Parameter Analysis in Visible Light Communications",
698 *31st Wireless and Optical Communications Conference (WOCC)*, Shenzhen, China, 11-12 August 2022.
- 699 28. Zhang, Long, Rui Jiang, Xinke Tang, Zhen Chen, Zhongyi Li, and Juan Chen. "Performance Estimation and Selection Guideline
700 of SiPM Chip within SiPM-Based OFDM-OWC System.", *MDPI Photonics*, **2022**, vol. 9, no. 9, p. 637.
- 701
- 702